Influence of one and two dimensional piezoelectric actuation on active vibration control of smart panels

S. Raja [a], P.K. Sinha [b], G. Prathap [c], P. Bhattacharya [a]

[a] *Structures Division, National Aerospace Laboratories (CSIR), Bangalore 560 017, India*
[b] *Department of Aerospace Engineering, Indian Institute of Technology, Kharagpur 721 302, India*
[c] *Centre for Mathematical Modelling and Computer Simulation (CSIR), Bangalore 560 037, India*

Abstract

The influence of directional piezoelectric actuation ($d_{31} \neq d_{32}$), and isotropic piezoelectric actuation ($d_{31} = d_{32}$) on static deflection and control behaviour of aluminium panels is evaluated through numerical experiments. A four-node *Piezo-Elastic* field consistent plate element based on Mindlin–Reissner theory is developed and the finite element procedure is implemented in MATLAB® platform. An active control scheme using Linear Quadratic Regulator is adopted in modal domain for the first mode control. The control analysis shows that the actuator efficiency is significantly modified with boundary effects. The directional actuation that actually represents the piezoelectric anisotropy has a better control performance compared to isotropic actuation. The results of the control study clearly indicate that if the d_{32}-based actuation effect is minimised then better control can be achieved.

Keywords: Directional actuation; Isotropic actuation; Active vibration control; Linear quadratic regulator (LQR); Independent Modal Space Control (IMSC)

1. Introduction

Active vibration control using piezoelectric materials as distributed actuators and sensors has been thoroughly studied and is widely accepted as an alternative approach to discrete active control system, as well as to passive control technology. The piezoelectric materials are also employed as actuators for static shape control applications [11,12, 19,20]. Finite element procedures to model the distributed actuation/sensing and experimental techniques to employ bonded/embedded piezoelectric layers in composites are also developed [4,15–17]. Benjeddou [2] has reviewed recently most of the works pertinent to finite element modelling of smart structures with piezoelectric layers.

The piezoelectric layer in a smart laminated composite is mostly considered as an orthorhombic crystal class, which has five piezoelectric constants [10]. In addition, the piezoelectric layer needs to be polarised along z-direction, so that it can be surface bonded or embedded into composite substrate easily (refer Fig. 1). A monolithic piezoelectric crystal polarised along z-direction, will have the same piezoelectric material properties in both transverse directions ($d_{31} = d_{32}$). Further, a discrete monolithic piezoelectric crystal attached conventionally (Conventionally Attached Piezo, CAP) on a substrate for vibration or shape control applications develops the actuation strains in both transverse directions equally. This type of actuation is known as isotropic actuation or two-dimensional actuation.

However, the effect of d_{32} actuation can be reduced or modified to introduce some percentage of piezoelectric anisotropy by directionally attaching the piezo crystal (Directionally Attached Piezo, DAP) on a substrate [1]. It is also possible to reduce the d_{32} based actuation effect in a discrete monolithic piezoelectric crystal by partially (for example 1/3rd of the width can be bonded from the centre of the crystal) bonding along its width. The resultant actuation strain will be developed mainly along the longitudinal direction and will be influenced by the piezoelectric constant d_{31}.

A more realistic way of achieving the piezoelectric anisotropy is demonstrated by Hagood et al. [3,9,18] by developing piezoelectric composite plies. Since the piezoelectric composite ply has the property $d_{31} \neq d_{32}$, a designer can introduce the piezoelectric anisotropic or orthotropic actuation in the smart laminated composites by properly orienting the active ply. The ideal piezoelectric anisotropic actuation can be simulated taking the value of d_{32} as zero, which represents pure uniaxial actuation case.

E-mail address: raja@css.cmmacs.ernet.in (S. Raja).

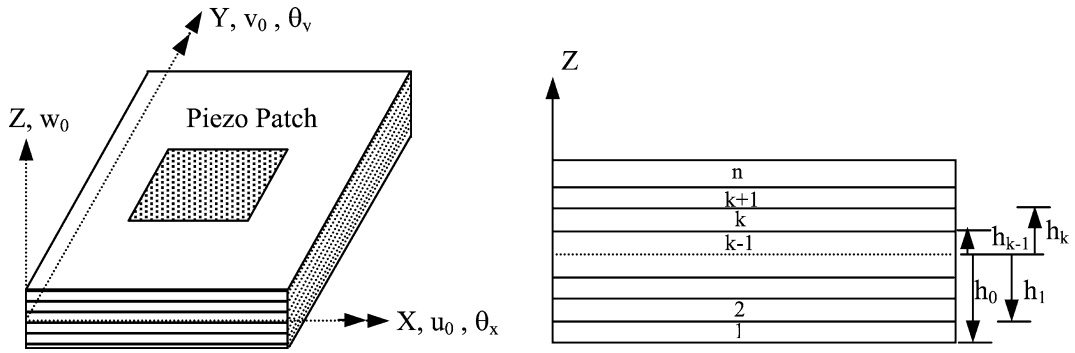

Fig. 1. Laminated plate configuration with surface bonded piezo patch.

Chee et al. [5] have studied the piezoelectric anisotropic actuation in composite plate structures using finite element method. A layerwise theory is used to define the electric potential variation across the thickness of the active layer and a third order displacement field model is employed for elastic field. The piezoelectric anisotropy is studied taking $d_{31} \neq d_{32}$ to evaluate the actuator performance.

Dimitriadis et al. [7] have addressed the two-dimensional actuation behaviour of the surface bonded piezoelectric patches on thin plates. The study shows that the two-dimensional actuator patch develops an equal amount of strain in both x and y directions due to piezoelectric constants $d_{31} = d_{32}$. Chee, Tong, and Steven [6] have reviewed the various aspects of modelling the piezoelectric sensor/actuator in intelligent structures including the non-linear models for piezoelectric coupling. Piezoelectric anisotropy is critically reviewed with directionally active piezoelectric composites.

Though extensive studies have been reported in the modelling of piezoelectric smart structures, the performance of isotropic actuation and anisotropic actuation, i.e. directional actuation need further investigation in the vibration control applications. In addition, the significance of directional actuation on the static deflection pattern is also an important aspect to realise the application of piezoelectric composites or directionally active piezoelectric (DAP) elements for static shape control. Therefore, the study on the influence of d_{31} alone (ideal piezoelectric anisotropy) and together with d_{32} (piezoelectric isotropy) on the converse piezoelectric coupling is carried out in the present investigation.

The present investigation considers an ideal piezoelectric anisotropy as one-dimensional actuation and it is a hypothetical case of unidirectional actuators. With this assumption, it is possible to represent the piezoelectric anisotropy presents in the piezoelectric composite ply or DAP element, by a thin monolithic piezo wafer in finite element modelling, giving only d_{31} value. As the piezoelectric composite ply has d_{32} value less than d_{31}, the active ply will develop mostly a directional actuation. Further, a comparison study is made with isotropic actuation, i.e. two-dimensional actuation to bring out the importance of piezoelectric anisotropy or directional actuation in vibration control application.

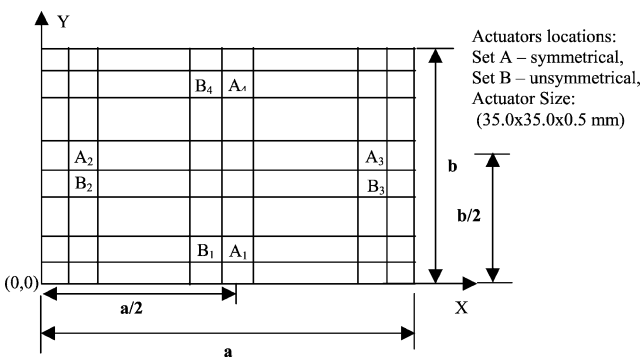

Fig. 2. Aluminium panel with actuator patch locations.

The proposed study involves structural modelling, controller design, open and closed loop systems response analysis on PC based MATLAB platform. A coupled piezoelectric finite element formulation of a laminated composite plate with embedded piezoelectric/piezoceramic materials is presented. A four-node Mindlin–Reissner plate element with mechanical displacement and electric potential as field variables is developed. The finite element analysis directly gives the actuator influence matrix and the sensor output vector, which can be used in the optimal controller design. An optimal controller based on Linear Quadratic Regulator (LQR) is designed using Independent Modal Space Control (IMSC) technique [8,13]. The aluminium panels ($a/b = 1.0$, 2.0 and $a/h = 435$) are considered as model problems for the vibration control study with the boundary conditions, (i) all edges clamped (C–C–C–C), and (ii) cantilevered (C–F–F–F). Actuators are placed at different locations (Set-A & Set-B) to find the influence of isotropic and directional actuation in controlling the first mode vibration (see Fig. 2).

2. Basic formulation

The virtual work done on a piezo-elastic body, if it behaves as an actuator, is derived from the stress equation of motion and is given by

$$\int_v (\rho \ddot{u}_j \delta u_j + \sigma_{ij} \delta \varepsilon_{ij})\, \mathrm{d}v = \int_v (f_{bj} \delta u_j)\, \mathrm{d}v + \int_s (f_{sj} \delta u_j)\, \mathrm{d}s \quad (1)$$

where u_j, σ_{ij}, ρ, ε_{ij}, f_{bj}, f_{sj}, are mechanical displacement, stress, density, strain, body force, and surface traction, respectively.

The virtual work done on a piezo-elastic body, if it behaves as a sensor, is obtained from the equation of electro statics and is defined as:

$$\int_v (D_j \delta \phi_{,j})\, \mathrm{d}v = \int_s (q \delta \phi)\, \mathrm{d}s, \quad (2)$$

where D_j, ϕ, q are electric flux density, scalar electric potential, and surface charge per unit area, respectively.

The strain field ε_{ij} and the electric field E_i are related to the displacement u and the scalar electric potential ϕ, respectively as follows:

$$\varepsilon_{ij} = \frac{1}{2}(u_{j,i} + u_{i,j}), \quad (3)$$

$$E_i = -\phi_{,i}. \quad (4)$$

The generalized weak form of coupled piezoelectric problem is derived using Eqs. (1)–(4), as:

$$\int_v (\rho \ddot{u}_i \delta u_i + \sigma_{ij} \delta \varepsilon_{ij} - D_i \delta E_i)\, \mathrm{d}v = \int_s f_{si} \delta u_i\, \mathrm{d}s + \int_s q \delta \phi\, \mathrm{d}s, \quad (5)$$

where the body force is not considered in the formulation.

The necessary coupling between the elastic and the electric fields is introduced by the linear constitutive relations [10].

$$\sigma_{ij} = c_{ijkl} \varepsilon_{kl} - d_{kij} E_k, \quad (6)$$

$$D_i = d_{ijk} \varepsilon_{kl} + \kappa_{ik} E_k, \quad (7)$$

where $c_{ijkl}, d_{kij}, \kappa_{ik}$, are the elastic, piezoelectric, and dielectric constants, respectively.

2.1. Lamina constitutive relations for extension–bending actuation

The stress–strain relationship is established with the assumption that the lamina is elastically orthotropic and piezoelectrically orthorhombic.

The lamina properties with respect to material axes are defined as follows:

$$\begin{Bmatrix} \sigma_{11} \\ \sigma_{22} \\ \tau_{23} \\ \tau_{13} \\ \tau_{12} \\ D_1 \\ D_2 \\ D_3 \end{Bmatrix} = \begin{bmatrix} Q_{11} & Q_{12} & 0 & 0 & 0 \\ Q_{12} & Q_{22} & 0 & 0 & 0 \\ 0 & 0 & Q_{44} & 0 & 0 \\ 0 & 0 & 0 & Q_{55} & 0 \\ 0 & 0 & 0 & 0 & Q_{66} \\ 0 & 0 & 0 & Q_{PE15} & 0 \\ 0 & 0 & Q_{PE24} & 0 & 0 \\ Q_{PE31} & Q_{PE32} & 0 & 0 & 0 \end{bmatrix} \begin{bmatrix} 0 & 0 & -Q_{PE31} \\ 0 & 0 & -Q_{PE32} \\ 0 & -Q_{PE24} & 0 \\ -Q_{PE15} & 0 & 0 \\ 0 & 0 & 0 \\ Q_{DE11} & 0 & 0 \\ 0 & Q_{DE22} & 0 \\ 0 & 0 & Q_{DE33} \end{bmatrix} \begin{Bmatrix} \varepsilon_{11} \\ \varepsilon_{22} \\ \gamma_{23} \\ \gamma_{13} \\ \gamma_{12} \\ E_1 \\ E_2 \\ E_3 \end{Bmatrix} \quad (8)$$

where

$$Q_{11} = C_{11} - \frac{C_{13}C_{13}}{C_{33}}; \qquad Q_{12} = C_{12} - \frac{C_{13}C_{23}}{C_{33}};$$

$$Q_{22} = C_{22} - \frac{C_{23}C_{23}}{C_{33}}; \qquad Q_{44} = C_{44}; \qquad Q_{55} = C_{55};$$

$$Q_{66} = C_{66}; \qquad Q_{PE31} = d_{31} - \frac{C_{13}d_{33}}{C_{33}};$$

$$Q_{PE32} = d_{32} - \frac{C_{23}d_{33}}{C_{33}}; \qquad Q_{PE24} = d_{24};$$

$$Q_{PE15} = d_{15}; \qquad Q_{DE11} = \kappa_{11};$$

$$Q_{DE22} = \kappa_{22}; \qquad Q_{DE33} = \kappa_{33} + \frac{d_{33}d_{33}}{C_{33}}.$$

The constitutive relationship in the X–Y–Z coordinate system can be obtained as follows:

$$\begin{Bmatrix} \sigma \\ D \end{Bmatrix}_{xyz} = [\,\overline{Q}\,] \begin{Bmatrix} \varepsilon \\ E \end{Bmatrix}_{xyz},$$

where $[\overline{Q}] = [T]^{\mathrm{T}}[Q][T]$, T is the transformation matrix.

3. Finite element formulation

Based on the first order shear deformation theory, the mechanical displacement fields are specified as:

$$\begin{aligned} u(x, y, z) &= u_0(x, y) + z\theta_y(x, y), \\ v(x, y, z) &= v_0(x, y) - z\theta_x(x, y), \\ w(x, y, z) &= w_0(x, y), \end{aligned} \quad (9)$$

where u_0, v_0, w_0, θ_x, θ_y, are the displacement components at the plate mid-plane [14].

Two multi-functional layers are considered in the formulation and they can be placed anywhere along the thickness direction of the laminate (kth layer, see Fig. 1). The active layers can be used either as actuators or as sensors in the distributed active control. The total electric potential in each active layer (subscript a-denotes actuator and s-denotes sensor) is given by:

$$\phi_a(x, y, z) = \phi_{0a}(x, y) + \frac{(z - h_{k-1})}{(h_k - h_{k-1})}\phi_{1a}(x, y),$$
$$\phi_s(x, y, z) = \phi_{0s}(x, y) + \frac{(z - h_{k-1})}{(h_k - h_{k-1})}\phi_{1s}(x, y), \tag{10}$$

where ϕ_0 is the mean electric potential defined at the mid-plane of the active layer and ϕ_1 is the difference of potential between top and bottom surfaces of the active layer. It is assumed that the electric potential variation across the thickness is linear because the multifunctional layer is relatively thin.

The linear gradient relations are described for mechanical and electric fields as follows:

$$\{\varepsilon\} = \{\varepsilon_{xx} \quad \varepsilon_{yy} \quad \gamma_{xy} \quad \gamma_{yz} \quad \gamma_{xz}\}^{\mathrm{T}} = \left\{ \frac{\partial u}{\partial x} \quad \frac{\partial v}{\partial y} \quad \frac{\partial u}{\partial y} + \frac{\partial v}{\partial x} \quad \frac{\partial v}{\partial z} + \frac{\partial w}{\partial y} \quad \frac{\partial u}{\partial z} + \frac{\partial w}{\partial x} \right\}^{\mathrm{T}}. \tag{11}$$

$$\{E\}_i = \{E_x \quad E_y \quad E_z\}^{\mathrm{T}} = \left\{ -\frac{\partial \phi_i}{\partial x} \quad -\frac{\partial \phi_i}{\partial y} \quad -\frac{\partial \phi_i}{\partial z} \right\}^{\mathrm{T}}, \quad i = a,\ s. \tag{12}$$

The elemental mechanical and electrical degrees of freedom fields are isoparametrically interpolated using linear shape functions.

$$\left\{u^e \phi^e\right\}^{\mathrm{T}} = \sum_{i=1,4} \mathrm{N}_i \{\bar{u}\ \bar{\phi}\}_i^{\mathrm{T}} \tag{13}$$

where $\{\bar{u}\} = \{u_0 \ v_0 \ w_0 \ \theta_x \ \theta_y\}^{\mathrm{T}}$, $\{\bar{\phi}\} = \{\phi_{1a} \ \phi_{1s}\}^{\mathrm{T}}$ are the nodal vectors of mechanical and electrical degrees of freedom, respectively and $N_i = 0.25(1 + \xi\xi_i)(1 + \eta\eta_i),\ i = 1, 4$.

Upon substituting Eqs. (9), (10), and (13) into gradient relations, we get:

$$\{\varepsilon\} = \sum_{i=1,4} [J]^{-1}[B_u]_i\{\bar{u}\}_i \quad \text{and}$$
$$\{E\} = \sum_{i=1,4} [J]^{-1}[B_\phi]_i\{\bar{\phi}\}_i \tag{14}$$

where $[J]$ is a Jacobian matrix and $[B_u]$, $[B_\phi]$, are the shape function derivative matrices of elastic and electric fields, respectively.

Using Eqs. (13), (14), together with the material constitutive relations, the energy equation is minimised for a stationary value to derive the governing FE equations in terms of nodal displacements and nodal voltages:

$$[M_{uu}]\{\ddot{\bar{u}}\} + [K_{uu}]\{\bar{u}\} + [K_{u\phi}]\{\bar{\phi}\} = \{F_m\}, \tag{15}$$
$$[K_{\phi u}]\{\bar{u}\} - [K_{\phi\phi}]\{\bar{\phi}\} = \{F_{\mathrm{el}}\}, \tag{16}$$

where F_m is the applied mechanical load and

$$[M_{uu}] = \int\int [N_u]^{\mathrm{T}}[\bar{\rho}][N_u]|J|\,\mathrm{d}\xi\,\mathrm{d}\eta;$$
$$[K_{uu}] = \int\int [B_u]^{\mathrm{T}}[\bar{c}][B_u]|J|\,\mathrm{d}\xi\,\mathrm{d}\eta;$$
$$[K_{u\phi}] = \int\int [B_u]^{\mathrm{T}}[\bar{d}][B_\phi]|J|\,\mathrm{d}\xi\,\mathrm{d}\eta;$$
$$[K_{\phi\phi}] = \int\int [B_u]^{\mathrm{T}}[\bar{\kappa}][B_\phi]|J|\,\mathrm{d}\xi\,\mathrm{d}\eta;$$
$$[K_{\phi u}] = [K_{u\phi}]^{\mathrm{T}};$$
$$\{F_{\mathrm{el}}\} = \frac{\kappa_{33}}{(h_k - h_{k-1})} \int\int [N_\phi]^{\mathrm{T}} V|J|\,\mathrm{d}\xi\,\mathrm{d}\eta.$$

Note that $[\bar{c}]$, $[\bar{d}]$, $[\bar{\kappa}]$, are the material constitutive matrices, $[\bar{\rho}]$ is the mass property matrix and the integration is carried out with limits -1 to $+1$. Eq. (16) is a general representation of direct piezoelectric effect, which contains the capacitance $(K_{\phi\phi})$, as well as equivalent charge generator $(K_{\phi u})$ matrices. It can be used to estimate the charge developed due to mechanical strain in the absence of applied electric field, i.e. F_{el} is equal to zero for sensor application.

4. State feedback control based on LQR/IMSC approach

In the present work, a state feedback optimal controller is designed in an infinite time domain. In the control scheme formulation, the system matrices, displacement and control vectors are presented using simple notations. The mathematical model of the 'active' panel is already given by Eq. (15) in matrix notation. However, for the sake of completeness, the dynamic equation is again presented with feedback control as

$$M_{uu}\ddot{\bar{u}} + C_{uu}\dot{\bar{u}} + K^*\bar{u} = F_m + K_a V_a, \tag{17}$$

where $K^* = K_{uu} + K_{u\phi}K_{\phi\phi}^{-1}K_{\phi u}$, is the condensed stiffness matrix, C_{uu} is a damping matrix, and $K_a = K_{u\phi}K_{\phi\phi}^{-1}F_a$, is the global actuator influence matrix in which matrix F_a relates the patch voltages V_a to nodal voltages.

The nodal voltages are related to the patch or element voltage for a four-node quadrilateral plate element as follows:

$$\left\{\bar{\phi}_{1a}(1)\ \bar{\phi}_{1a}(2)\ \bar{\phi}_{1a}(3)\ \bar{\phi}_{1a}(4)\right\}^{\mathrm{T}} = [N_1\ N_2\ N_3\ N_4]^{\mathrm{T}} V_a, \tag{18}$$

and

$$F_a^e = \frac{\kappa_{33a}}{t_a} \int\int [N_1\ N_2\ N_3\ N_3]^{\mathrm{T}}|J|\,\mathrm{d}\xi\,\mathrm{d}\eta.$$

The element matrix F_a^e is formulated in the finite element analysis for each active element taking unit patch voltage and the element matrices are assembled to get global patch voltage matrix F_a.

Independent Modal Space Control (IMSC) is a modal filter approach to transfer the responses of multi degrees of freedom system into independent modal coordinates. Using the IMSC concept, the feedback control force is made independent (as a function of modal coordinates) completely to decouple the structural modes in a feedback control environment. Further, an optimal controller (LQR) can be designed using the modal control concept to individually control any structural mode.

The system is first solved for the free vibration analysis without damping.

Thereafter the dynamic equation is reduced to modal form using the following transformation,

$$\bar{u} = \Phi r \tag{19}$$

where Φ is a modal matrix containing the eigen vector of the open-loop system, normalised with respect to mass and r is modal coordinates.

The equation of motion is decoupled using the modal matrix and is presented here in modal form with feedback control as:

$$\ddot{r}_i + \overline{C}\dot{r}_i + \overline{K} r_i = b V_a, \quad i = 1, 2, \ldots, n \text{ modes}, \tag{20}$$

where

$$\overline{M} = \Phi^{\mathrm{T}} M_{uu} \Phi = \text{Identity matrix};$$
$$\overline{C} = \Phi^{\mathrm{T}} C_{uu} \Phi = \operatorname{diag}(2\zeta_i \omega_i);$$
$$\overline{K} = \Phi^{\mathrm{T}} K^* \Phi = \operatorname{diag}\left(\omega_i^2\right) \quad \text{and} \quad b = \Phi^{\mathrm{T}} K_a.$$

A state vector η containing modal displacement and modal velocity is defined using two new states x_1 and x_2 as:

$$\eta_i = \begin{Bmatrix} r_i \\ \dot{r}_i \end{Bmatrix} = \begin{Bmatrix} x_1 \\ x_2 \end{Bmatrix}; \quad \ddot{r}_i = \dot{x}_2 \quad \text{and} \quad \dot{x}_1 = \dot{r}_i = x_2. \tag{21}$$

The modal state-space equation is obtained using Eqs. (20), (21), and is given bellow:

$$\dot{\eta}_i = A_i \eta_i + B_i V_{ai}, \tag{22}$$

where the matrices A_i is of size (2×2), B_i is of size $(2 \times a)$, for the ith mode and a is the number of actuator patches.

In addition, the corresponding block diagonals are [8],

$$[A_i] = \begin{bmatrix} 0 & 1 \\ -\omega_i^2 & -2\zeta\omega_i \end{bmatrix}; \qquad [B_i] = \begin{bmatrix} 0 \\ b(i,a) \end{bmatrix}. \tag{23}$$

In the present analysis, the following linear control law is adopted for the first mode vibration control:

$$V_{ai} = -G_i \eta_i, \tag{24}$$

where G_i is the optimal modal gain and note that the feedback voltage is proportional to the state vector.

We seek the optimal modal feedback gain such that the feedback control law (Eq. (24)) minimises the modal performance index:

$$J_i = \int_0^\infty \left(\eta_i^{\mathrm{T}} Q_i \eta_i\right) + \left(V_{ai}^{\mathrm{T}} R_i V_{ai}\right) \mathrm{d}t \to \min, \tag{25}$$

where Q_i is the state penalty matrix and R_i is the control penalty matrix.

The modal steady state solution S_i is obtained by solving the following Arithmetic Riccati Equation:

$$0 = S_i A_i + A_i^{\mathrm{T}} S_i - S_i B_i R_i^{-1} B_i^{\mathrm{T}} S_i + Q_i. \tag{26}$$

The optimum modal gain in steady state is then expressed as:

$$G_i = R_i^{-1} B_i^{\mathrm{T}} S_i. \tag{27}$$

Eqs. (26) and (27) are solved using MATLAB function (LQR) and the results are obtained for different cases.

5. Results and discussion

The developed FE procedure in the earlier section for the analysis of smart plate like structure is coded in MATLAB as M-files. The active modal control scheme is then implemented using the in-built M-files (LQR, DAMP, EIG etc.) in the control toolbox. The focus of the present study is to understand the behaviour of one-dimensional (directional actuation) and two-dimensional (isotropic actuation) piezoelectricity on the static and control behaviour of plate type structures. The aluminium panels of size 0.5×0.5 m (square) and 0.5×0.25 m (rectangular) with surface bonded piezoelectric (PZT) patches are considered in the numerical analysis.

The material properties are:

$E_{\mathrm{AL}} = 70$ GPa, $\quad \nu_{\mathrm{AL}} = 0.3$, $\quad \rho_{\mathrm{AL}} = 2800$ Kg/m^3,

$E_{\mathrm{PZT}} = 79$ GPa, $\quad \nu_{\mathrm{PZT}} = 0.3$, $\quad \rho_{\mathrm{PZT}} = 7800$ Kg/m^3,

d_{31}, d_{32} (Piezoelectric strain constant)

$= 1.428 \times 10^{-10}$ m/V,

κ (Electric permitivity) $= 1.65 \times 10^{-8}$ F/m.

The structural boundary conditions, namely clamped (all four edges constrained, C–C–C–C) and cantilever (one edge constrained, C–F–F–F) are considered. The square panel $(a/b = 1)$ is idealised with 13×13 mesh and the rectangular panel $(a/b = 2)$ is discretised with 13×7 mesh.

5.1. Static piezoelectric coupling analysis

5.1.1. Clamped plates

The aluminium panel $(a/b = 1.0)$ is subjected to a unit potential on all the four patches (set-A). Fig. 3 shows the transverse static displacement pattern due to one-dimensional (d_{31}) and two-dimensional $(d_{31} = d_{32})$ piezoelectric actuation along X-axis (i.e. line $Y = b/2$) and along Y-axis (i.e. line $X = a/2$). It is observed that the transverse displacement pattern for one-dimensional and two-dimensional effect is more or less same but the magnitude is more in the case of two-dimensional actuation. Moreover, this is more significant along the Y-axis. The bending stresses (σ_{xx} and σ_{yy}) are also obtained and are presented in Table 1. It can be seen that the bending stress along X-axis (σ_{xx}) for one- and two-dimensional piezoelectric actuation is comparable, whereas, the stress along Y-axis for two-dimensional piezoelectric actuation is almost fifteen times higher than one-dimensional actuation. The same trend is observed for the panel $(a/b = 2.0)$ and the results are presented in Table 2 and in Fig. 4.

5.1.2. Cantilever plate

In this example, a cantilever square panel $(a/b = 1.0,$ $a/h = 435)$ with four surface bonded piezo (PZT) patches

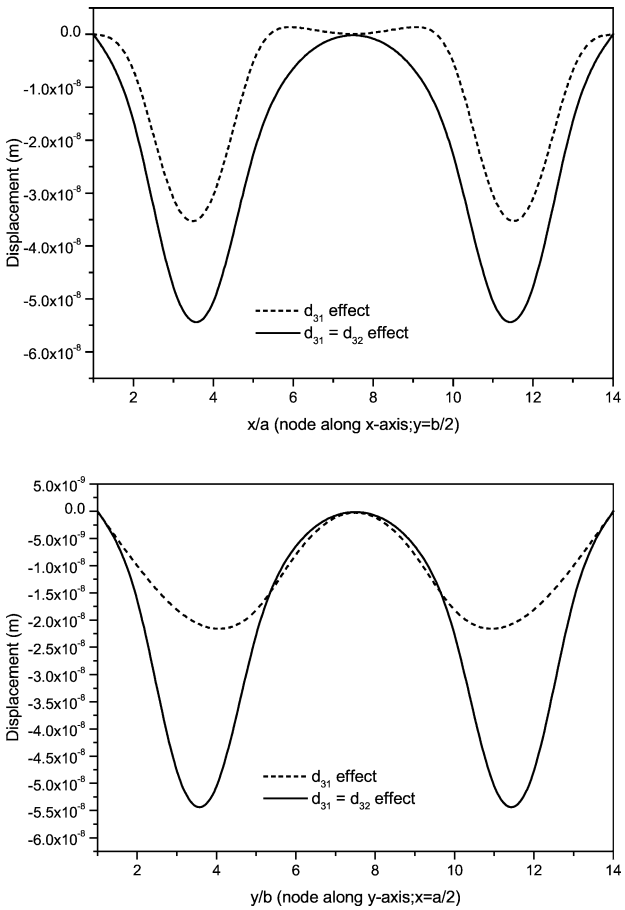

Fig. 3. Transverse displacement along X-axis and Y-axis of an aluminium panel ($a/b = 1.0$; $a/h = 435$, C–C–C–C) subjected to unit voltage applied on PZT patch set-A.

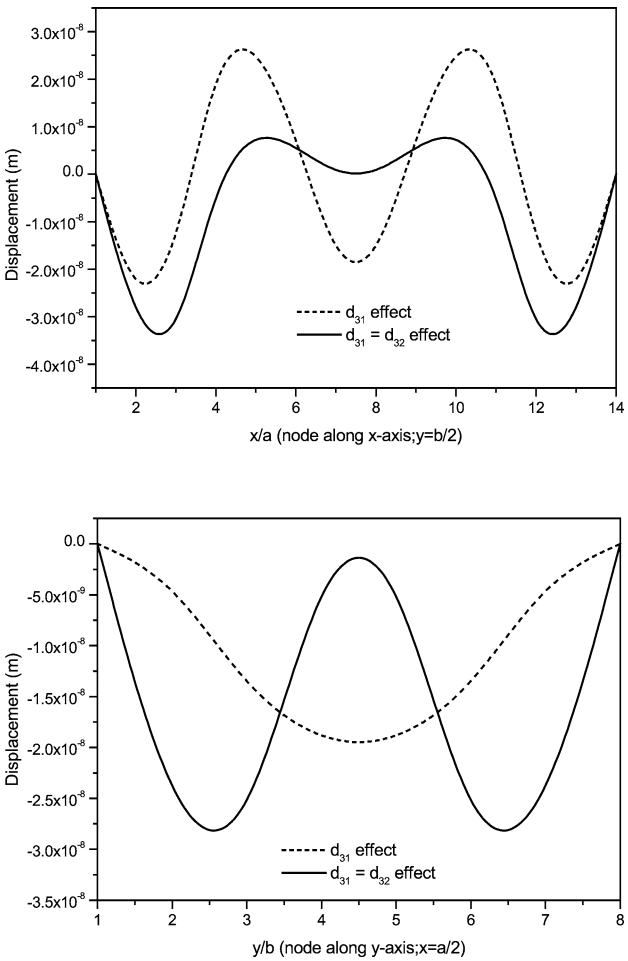

Fig. 4. Transverse displacement along X-axis and Y-axis of an aluminium panel ($a/b = 2.0$; $a/h = 435$, C–C–C–C) subjected to unit voltage applied on PZT patch set-A.

Table 1
Stresses developed due to 1-D and 2-D piezoelectric actuation in the actuator patches of an aluminium C–C–C–C panel for 1 V ($a/b = 1.0$, $a/h = 435$)

Patch no	d_{31} effect		$d_{31} = d_{32}$ effect	
	σ_{xx}	σ_{yy}	σ_{xx}	σ_{yy}
	(N/M^2)		(N/M^2)	
A1	2.4236e+3	1.6888e+2	2.5042e+3	2.4552e+3
A2	2.3576e+3	1.5318e+2	2.4552e+3	2.5042e+3
A3	2.3576e+3	1.5318e+2	2.4552e+3	2.5042e+3
A4	2.4236e+3	1.6888e+2	2.5042e+3	2.4552e+3

Table 2
Stresses developed due to 1-D and 2-D piezoelectric actuation in the actuator patches of an aluminium C–C–C–C panel for 1 V ($a/b = 2.0$, $a/h = 435$)

Patch no	d_{31} effect		$d_{31} = d_{32}$ effect	
	σ_{xx}	σ_{yy}	σ_{xx}	σ_{yy}
	(N/M^2)		(N/M^2)	
A1	2.2590e+3	2.6983e+2	2.4234e+3	2.3273e+3
A2	2.2533e+3	2.1013e+2	2.4056e+3	2.5415e+3
A3	2.2533e+3	2.1013e+2	2.4056e+3	2.5415e+3
A4	2.2590e+3	2.6983e+2	2.4234e+3	2.3273e+3

is considered to study the influence of one and two-dimensional piezoelectric actuation on the static deformation behaviour. The piezo patches (set-A) are subjected to a unit potential and the estimated displacements are plotted in Fig. 5 (along X-axis, $Y = b/2$ and along Y-axis, $X = a$). It is observed that the displacement obtained for one-dimensional piezoelectric effect is more than that of two-dimensional effect. In case of two-dimensional piezoelectric actuation, extensional behaviour is observed in both X- and Y-direction. The piezoelectric extensional effect in the Y-direction generates counteracting moment that in turn reduces the transverse deflection along the X-axis.

5.2. Modal control analysis

A modal response analysis is carried out on the aluminium panels using the Newmark time integration approach with sinusoidal disturbance, applied at the centre of the panels. The control performance due to directional actuation (d_{31}) is evaluated and a comparison with isotropic actuation ($d_{31} = d_{32}$) is made using the developed control scheme. In both the cases, the weighting factor for the

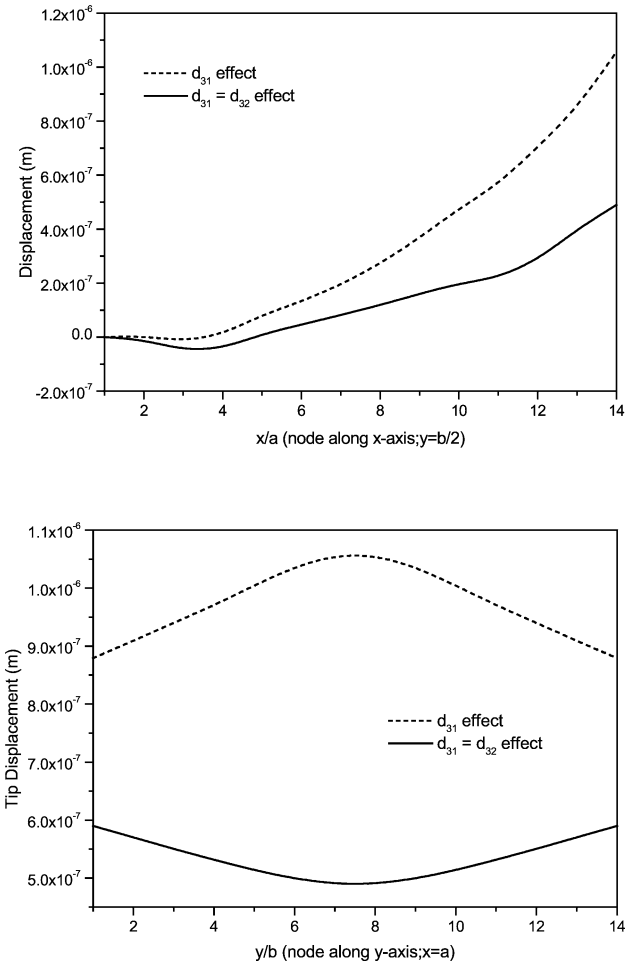

Fig. 5. Transverse displacement along X-axis and Y-axis of an aluminium panel ($a/b = 1.0$; $a/h = 435$, C–F–F–F) subjected to unit voltage applied on PZT patch set-A.

Table 3
Effect of 1-D and 2-D piezoelectric actuation on damped frequency in the first mode control of an aluminium C–C–C–C panel ($a/b = 1.0, a/h = 435$)

Weighting factor (R)	d_{31} effect		$d_{31} = d_{32}$ effect	
	Set-B ω_d (rad/sec)	Set-A ω_d (rad/sec)	Set-B ω_d (rad/sec)	Set-A ω_d (rad/sec)
1.0e−7	250.567	249.302	250.562	249.296
1.0e−8	250.554	249.287	250.556	249.289
1.0e−9	250.417	249.142	250.493	249.224
1.0e−10	249.407	247.685	249.861	248.567
1.0e−11	234.901	232.613	243.453	241.909
1.0e−12	Unstable	Unstable	Unstable	Unstable

control variable (R) is varied to apply different control effort. The C–C–C–C aluminium square panel is taken as an example to explain the influence of both one- and two-dimensional actuation on the first mode control. The first mode frequency of the panel (open-loop system) with actuators set-A is $f = 249.31$ Hz; and with set-B is $f = 250.58$ Hz, and the control analysis results are presented in Table 3 for various weighting factors. It is observed that be-

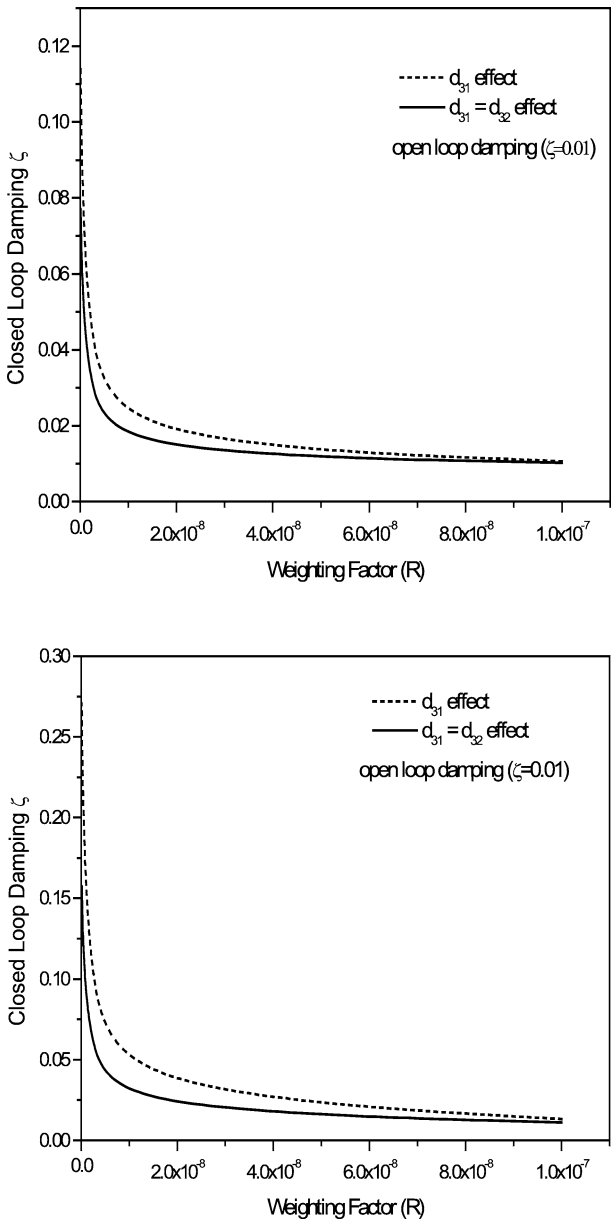

Fig. 6. Influence of control penalty parameter (R) on the closed loop performance of smart square panels with C–C–C–C and C–F–F–F edges (set-A).

yond a certain value of the weighting factor ($R = 1.0\,\mathrm{e}^{-10}$) the system performance in terms of damping increases but one has to pay a penalty in terms of structural frequencies. It is also found that the active damping (ς) introduced by directional actuation is more compared to isotropic actuation (see Fig. 6). The observed trend clearly shows that if the d_{32}-based actuation effect is reduced or minimised then better control can be achieved. The peak-to-peak actuator voltage with proper phase information for directional and isotropic actuation is presented in Table 4. It is also noted that for directional piezoelectric effect, the symmetrically placed piezo patches behave in a similar fashion whereas,

Table 4
Effect of 1-D and 2-D piezoelectric actuation on actuator patch voltages in the first mode control of an aluminium C–C–C–C panel ($a/b = 1.0, a/h = 435$)

Weighting factor (R)	d_{31} effect						$d_{31} = d_{32}$ effect		
	Patch voltages (V)						Patch voltages (V)		
	$A1$, $A4$ (+)	$A2$, $A3$ (−)	$B1$ (+)	$B2$ (−)	$B3$ (−)	$B4$ (+)	A	$B1$, $B4$	$B2$, $B3$
							(all actuators in-phase)		
1.0e−7	3.2	1.6	3.0	1.4	1.6	3.2	1.6	1.6	1.8
1.0e−8	24.0	12.0	24.0	11.0	13.0	24.0	14.0	14.0	16.0
1.0e−9	100.0	48.0	98.0	45.0	50.0	100.0	74.0	76.0	84.0
1.0e−10	190.0	94.0	196.0	90.0	98.0	200.0	180.0	192.0	214.0
1.0e−11	240.0	116.0	240.0	110.0	120.0	246.0	250.0	260.0	290.0

for bi-directional piezoelectric effect all the four actuators behave similarly.

6. Conclusions

A study is carried out to find the influence of directional and isotropic actuation on the static deflection and the vibration control behaviour of isotropic plates with various boundary conditions. A four-node plate finite element with structural-piezoelectric coupling is developed and implemented in MATLAB environment. It is observed that the stress pattern and the deflection behaviour for static analysis show significant difference with the piezoelectricity behaviour. This pattern is more significant for cantilever plate. An IMSC based LQR feedback control strategy is used to actively control the vibration of isotropic plates with surface bonded piezoceramic actuators. It is interesting to note that the directional piezoelectric actuation shows greater damping coefficient for the same control effort as compared to isotropic actuation. This trend is same for both clamped as well as cantilever plate configuration. It clearly shows that if the d_{32}-based actuation effect is reduced as much as possible then better control can be achieved.

References

[1] R. Barrett, Active plate and wing research using EDAP elements, Smart Materials and Structures 1 (1992) 214–226.
[2] A. Benjeddou, Advances in piezoelectric finite element modelling of adaptive structural elements: A survey, Computers and Structures 76 (2000) 347–363.
[3] A.A. Bent, N.W. Hagood, J.P. Rodgers, Anisotropic actuation with piezoelectric fibre composites, J. Intelligent Material Systems and Structures 6 (1995) 338–349.
[4] P. Bhattacharya, A. Suhail, P.K. Sinha, Finite element free vibration analysis of smart laminated composite beams and plates, J. Intelligent Material Systems and Structures 9 (1998) 20–28.
[5] C. Chee, L. Tong, G. Steven, A mixed model for adaptive composite plates with piezoelectric for anisotropic actuation, Computers and Structures 77 (2000) 253–268.
[6] Y.K. Clinton, C. Chee, L. Tong, G.P. Steven, A review of the modelling of piezoelectric sensors and actuators incorporated in intelligent structures, J. Intelligent Material Systems and Structures 9 (1998) 3–19.
[7] E.K. Dimitriadis, C.R. Fuller, C.A. Rogers, Piezoelectric actuators for distributed vibration excitation of thin plates, J. Vibration and Acoustics 113 (1991) 100–107.
[8] W.K. Gawronski, Dynamics and Control of Structures – A Modal Approach, Springer-Verlag, New York, 1998.
[9] N.W. Hagood, A.A. Bent, Development of piezoelectric fiber composites for structural actuation, in: Structural Dynamics and Materials Conference (Collection of Technical Papers AIAA/ASME Structures), Part 6, AIAA, 1993, pp. 3625–3638.
[10] IEEE Standard on Piezoelectricity, ANSI/IEEE Std 176-1978.
[11] D.B. Koconis, L.P. Kollár, G.S. Springer, Shape control of composite plates and shells with embedded actuators-I voltages specified, J. Composite Materials 28 (5) (1994) 415–457.
[12] C.C. Lin, C.Y. Hsu, H.N. Huang, Finite element analysis on deflection control of plates with piezoelectric actuators, J. Composite Structures 35 (1996) 423–433.
[13] L. Meirovitch, Dynamics and Control of Structures, John Wiley & Sons, 1990.
[14] G. Prathap, The Finite Element Method in Structural Mechanics, Kluwer Academic Publishers, Dordrecht, 1993.
[15] S. Raja, M. Rose, D. Sachau, Finite element model for intelligent plate structures involving multi-field coupling and experimental validation, IB 131-99/14, 1999, DLR-Institute of Structural Mechanics, Braunschweig, Germany.
[16] S. Raja, P. Bhattacharya, R. Balasubramaniam, Active Vibration Control of a Smart Panel Using LQR/IMSC Controller, Proc. of VETOMAC-I, IISc, Bangalore, India, 2000.
[17] S. Raja, K. Rohwer, M. Rose, Piezothermoelastic modelling and active vibration control of laminated piezoelectric composite beam, J. Intelligent Material Systems and Structures 10 (11) (1999) 890–899.
[18] J.P. Rodgers, N.W. Hagood, Manufacture of Adaptive Composite Plates Incorporating Piezoelectric Fiber Composite Plies, AIAA-95-1096-CP, 2824–2835.
[19] D. Tong, R.L. Williams II, Optimal shape control of composite thin plates with piezoelectric actuators, J. Intelligent Material Systems and Structures 9 (1998) 458–467.
[20] S. Varadarajan, K. Chandrashekhara, Adaptive Shape Control of Laminated Composite Plates Using Piezoelectric Materials, AIAA-96-1288-CP, 197–206.